Supplemental Material

Developmental regulation of $p66^{Shc}$ is altered by bronchopulmonary dysplasia in baboons and humans

Matt K. Lee, Gloria S. Pryhuber, Margaret A. Schwarz, Susan M. Smith, Zdena Pavlova, Mary E. Sunday

Figure Legends

Figure E1

Western analysis demonstrates Shc isoform regulation during baboon lung development and induction of BPD. Lysates from normal and premature baboons were equalized by total protein content and subjected to Shc Western analysis. Lanes marked * and # are identical samples loaded onto different blots to permit quantitation across different membranes. (A), fetal baboon lungs, (B), GAPDH reprobe of (A). Precipitous decline in GAPDH reactivity after birth is noted. Loading is otherwise equivalent. (C), 125 day baboons maintained on a mildly fibrotic BPD protocol. Animals were exposed to minimal O_2 as clinically indicated. (D), GAPDH reprobe of (C) showing equivalent loading. (E), additional gestational control specimens included in analysis. (F) total protein content of (E) demonstrating equivalent loading,

Figure E2

Minimal PARP proteolysis was noted at any stage of baboon lung development. Sections were subjected to $p66^{Shc}$ and cleaved PARP immunohistochemistry (green and red, respectively). Sections were obtained from baboons at 60 days gestation (A), 90 days gestation (B), 125 days gestation (C), 175 days gestation (D), and 3 days after term delivery at 185 days (E). Minimal cleaved PARP immunoreactivity was identified.

Figure E3

Minimal PARP proteolysis was noted in the 125 day baboon BPD model. $p66^{Shc}$ and cleaved PARP

(green and red, respectively) were immunolocalized in lungs from fetal baboons at 125 days gestation or identical animals maintained for 14 days *ex utero* with supplemental oxygen only as clinically indicated. Minimal cleaved PARP reactivity was noted. Mesenchymal $p66^{Shc}$ localization in the 125 day gestational control lung (C) was confirmed co-immunolocalizing $p66^{Shc}$ (green) and cytokeratin (red). Epithelial cells are labeled by anti-pan-cytokeratin antibody (Sigma). In contrast, 125 day animals maintained for 14 days *ex utero* demonstrated widespread epithelial localization (D). Co-immunolocalization of $p66^{Shc}$ (green) and α-smooth muscle actin (red) indicated minimal co-localization in either 125 day gestational controls (E) or animals maintained for 14 days *ex utero.* Smooth muscle actin is expressed by myofibroblasts, airway smooth muscle, and vascular smooth muscle. Specificity was confirmed by probing otherwise identically processed sections were with anti-$p66^{Shc}$ antibody preadsorbed to the immunizing peptide.

Figure E4

Regulated tissue localization of $p66^{Shc}$ in the 140 day fetal baboon BPD model was confirmed by co-localization with cytokeratin. Epithelial cells are labeled red by anti-pan-cytokeratin antibody while $p66^{Shc}$ is labeled green. In 140 day gestational controls, $p66^{Shc}$ is expressed in both epithelial and mesenchymal cells (A). Animals exposed to supplemental O_2 for 10 days only as clinically indicated (B) developed minimal fibrosis and $p66^{Shc}$ localization similar to that of 140 day gestational controls. In contrast, 140 day animals exposed to 100% O_2 for 10 days expressed $p66^{Shc}$ in clusters of mesenchymal cells within fibrotic interalveolar septa (C). The clinical and pathological severity of BPD in this model is attenuated by infusion of the anti-BLP antibody 2A11. Animals treated with 100% O_2 and 2A11 (D) retained epithelial $p66^{Shc}$ expression. Similarly, $p66^{Shc}$ also localized to the epithelium of normal 160 day baboon lungs (E). Specificity was confirmed by probing otherwise

identically processed sections with anti-p66^{Shc} antibody preadsorbed to the immunizing peptide.

Figure E5

Cells expressing p66^{Shc} tended not to co-express α-smooth muscle actin in the 140 day baboon BPD model. p66^{Shc} is labeled green and α-smooth muscle actin is labeled red. (A), 140 day gestational controls; (B), 140 day animals exposed to minimal supplemental O_2; (C) 140 day animals exposed to 100% O_2 for 10 days; (D) 140 day animals exposed to 100% O_2 for 10 days while infused with 2A11 antibody; (E) 160 day gestational controls. Even when expressed primarily in the mesenchyme, high level p66^{Shc} expression rarely coincided with α-smooth muscle actin localization. Preadsorbed controls are the same as in Figure E3.

Figure E6

Western analysis demonstrates developmental p66^{Shc} regulation in fetal human lungs. (A), Western blot from which Figure 7 was excerpted. All lanes are loaded with 30 Fg total protein. Quantitation was performed directly without normalization. (B), reprobe of the same blot with anti-glyceraldehyde phosphate dehydrogenase (GAPDH) antibody. A sharp decrease in GAPDH expression after 20 weeks was evident. (C), colloidal gold staining of the same blot demonstrated equivalent overall protein content in each lane.

Figure E7

Tissue localization of p66^{Shc} is modulated during human lung development, as confirmed by cytokeratin co-immunolocalization. Lung sections from normal human fetuses were immunostained for p66^{Shc} (green) and cytokeratin (red). Epithelial populations were labeled by anti-pan-cytokeratin

antibody. Expression of $p66^{Shc}$ was widespread throughout the 18 week lung, and especially prominent in the epithelium (A). At 20 weeks (B), epithelial expression remained strong while mesenchymal expression had diminished. At 22 weeks (C), $p66^{Shc}$ had decreased further and high-level expression was restricted to occasional cells in both the epithelial and mesenchymal compartments. By 24 weeks (D), much of the mesenchyme had involuted and relatively few epithelial cells continued to express high levels of $p66^{Shc}$. Specificity was confirmed by probing otherwise identically processed sections with anti-$p66^{Shc}$ antibody preadsorbed to the immunizing peptide.

Figure E8

Contractile cells in the developing human lung do not appear to express $p66^{Shc}$. $p66^{Shc}$ is labeled green and α-smooth muscle actin is labeled red. Myofibroblasts, airway smooth muscle, and perivascular smooth muscle cells contain α-smooth muscle actin. (A), 18 week human lung; (B), 20 week lung; (C) 22 week lung; and (D) 24 week lung. High level $p66^{Shc}$ expression rarely coincides with α-smooth muscle actin localization. Preadsorbed controls are the same as in Figure E6.

Figure E9

Apoptosis is not clearly related to $p66^{Shc}$ expression in developing human lung. Cleaved PARP expression is an early marker of apoptosis. Lung sections were co-immunostained for $p66^{Shc}$ (green) and cleaved PARP (red). In the 18 week lung (A), occasional areas of cleaved PARP were noted in the mesenchyme, but no clear association with $p66^{Shc}$ expression could be discerned. In the 20 week lung (B), PARP cleavage had diminished while $p66^{Shc}$ remained relatively abundant. Subsequently, PARP proteolysis was undetectable in the 22 week (C) and 24 week (D) human lung. Specificity was confirmed by probing otherwise identically processed sections with $p66^{Shc}$ antibody preadsorbed to the

immunizing peptide.

Figure E10

The tissue localization of $p66^{Shc}$ is modulated by induction of BPD in human neonates. Pathological sections were immunostained for $p66^{Shc}$ (green) and cytokeratin (red). Autopsies were performed within 6 hours of death, and clinical synopses are listed in Table 1. In near-term newborn infants without lung disease, (A, Case 2, 4 day old ex-36 week infant), nearly all cells expressed some $p66^{Shc}$. However, more intensely labeled cells was scattered throughout the mesenchyme. Newborn preterm infants had thicker septa (B, Case 9, 1 day old ex-27 week infant) than term newborns. Moderate levels of $p66^{Shc}$ were present in most mesenchymal cells, and high-level expression was apparent in scattered epithelial cells. Older premature infants without BPD (C, Case 10, 32 day old ex-28 week infant) had thinner interalveolar septa, but continued to exhibit moderate $p66^{Shc}$ labeling of most mesenchymal cells and increased expression within scattered epithelial cells. In contrast, the lungs of a 13 day old ex-28 week infant with early evolving BPD (D, Case 7) had thickened septa, heterogeneously labeled mesenchymal cells, and continuous lines of labeled epithelial cells. In an older patient with mildly fibrotic BPD (E, Case 5, 60 day old-ex 26 week infant), $p66^{Shc}$ localized to continuous lines of strongly expressing epithelial cells. As in early BPD, the mesenchymal compartment was heterogeneously labeled. In contrast, the patient with severe fibrotic BPD (F, Case 4, 97 day old ex-27 week infant) expressed $p66^{Shc}$ primarily in the mesenchyme, with relatively little epithelial expression.

Figure E11

$p66^{Shc}$ is not strongly expressed by contractile cells in lungs with BPD. Pathological sections were

immunostained for $p66^{Shc}$ (green) and α-smooth muscle actin (red). Smooth muscle actin is expressed by myofibroblasts, airway smooth muscle, and vascular smooth muscle (A), Case 2, 4 day old ex-36 week infant without lung disease; (B), Case 9, 1 day old ex-27 week infant; (C), Case 10, 32 day old ex-28 week infant without BPD; (D), 13 day old ex-28 week premature infant with early evolving BPD; (E), Case 5, 60 day old-ex 26 week infant), an older patient with mildly fibrotic BPD; and (F), Case 4, 97 day old ex-27 week infant, a patient with a clinical course consistent with classical severe fibrotic BPD. Cells expressing $p66^{Shc}$ tended not to express α-smooth muscle actin.

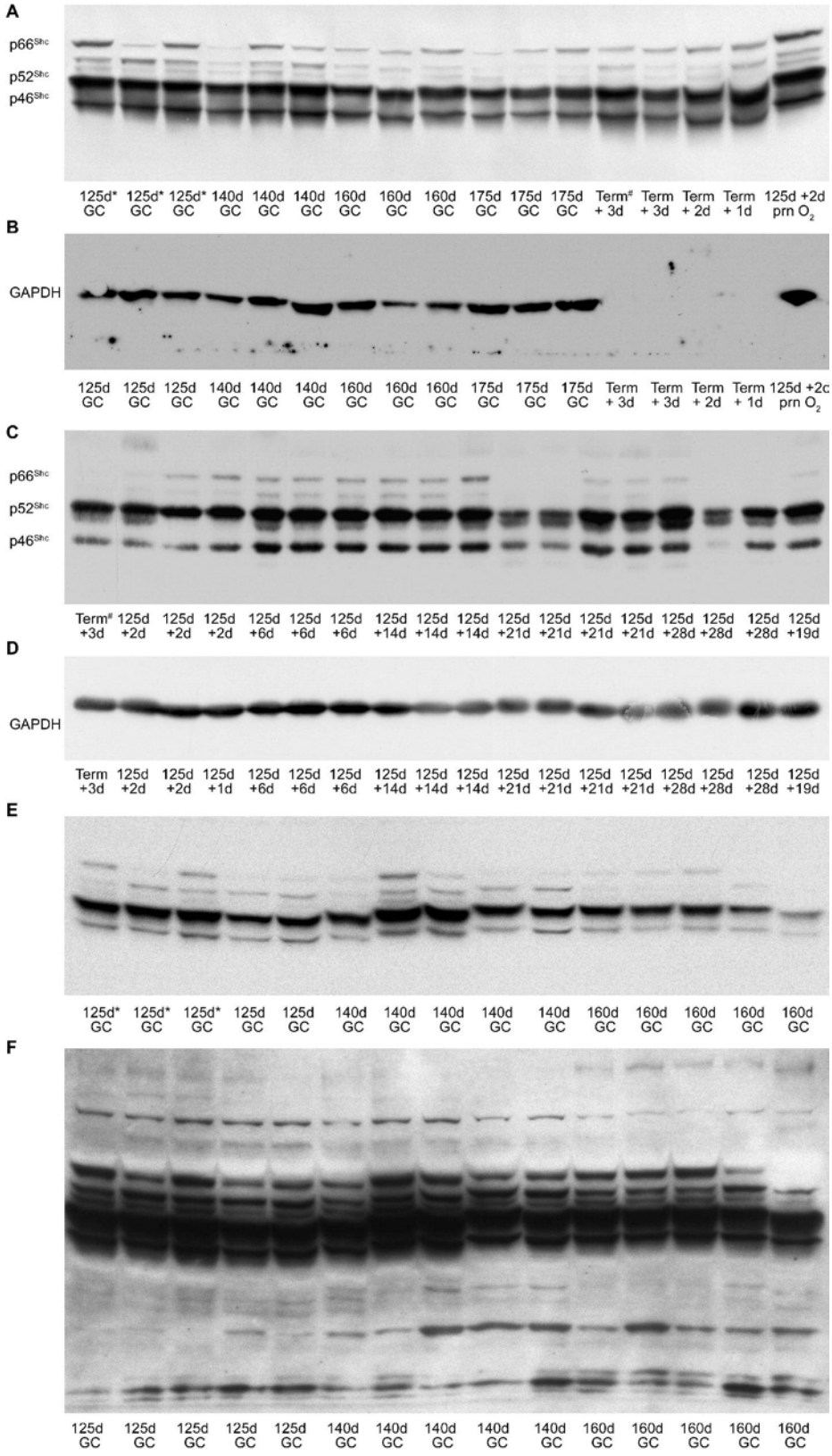
A
p66Shc
p52Shc
p46Shc
125d* GC 125d* GC 125d* GC 140d GC 140d GC 140d GC 160d GC 160d GC 160d GC 175d GC 175d GC 175d GC Term# + 3d Term + 3d Term + 2d Term + 1d 125d prn O2 +2d
B
GAPDH
125d GC 125d GC 125d GC 140d GC 140d GC 140d GC 160d GC 160d GC 160d GC 175d GC 175d GC 175d GC Term + 3d Term + 3d Term + 2d Term + 1d 125d prn O2 +2c
C
p66Shc
p52Shc
p46Shc
Term# +3d 125d +2d 125d +2d 125d +2d 125d +6d 125d +6d 125d +6d 125d +14d 125d +14d 125d +14d 125d +21d 125d +21d 125d +21d 125d +21d 125d +28d 125d +28d 125d +28d 125d +19d
D
GAPDH
Term +3d 125d +2d 125d +2d 125d +1d 125d +6d 125d +6d 125d +6d 125d +14d 125d +14d 125d +14d 125d +21d 125d +21d 125d +21d 125d +21d 125d +28d 125d +28d 125d +28d 125d +19d
E
125d* GC 125d* GC 125d* GC 125d GC 125d GC 140d GC 140d GC 140d GC 140d GC 140d GC 160d GC 160d GC 160d GC 160d GC 160d GC
F
125d GC 125d GC 125d GC 125d GC 125d GC 140d GC 140d GC 140d GC 140d GC 140d GC 160d GC 160d GC 160d GC 160d GC 160d GC

Figure E1

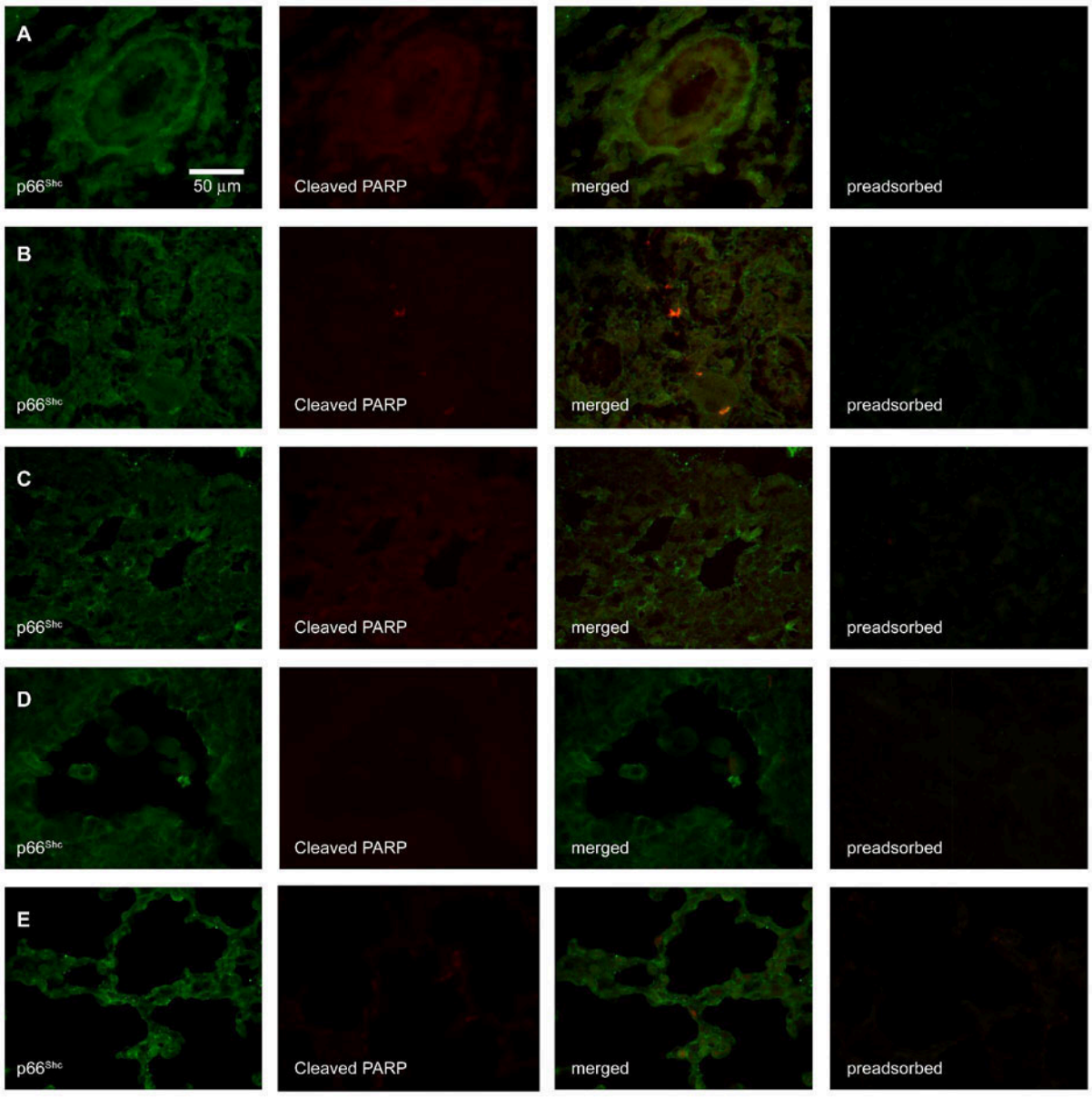
A
p66Shc
50 µm
Cleaved PARP
merged
preadsorbed
B
p66Shc
Cleaved PARP
merged
preadsorbed
C
p66Shc
Cleaved PARP
merged
preadsorbed
D
p66Shc
Cleaved PARP
merged
preadsorbed
E
p66Shc
Cleaved PARP
merged
preadsorbed

Figure E2

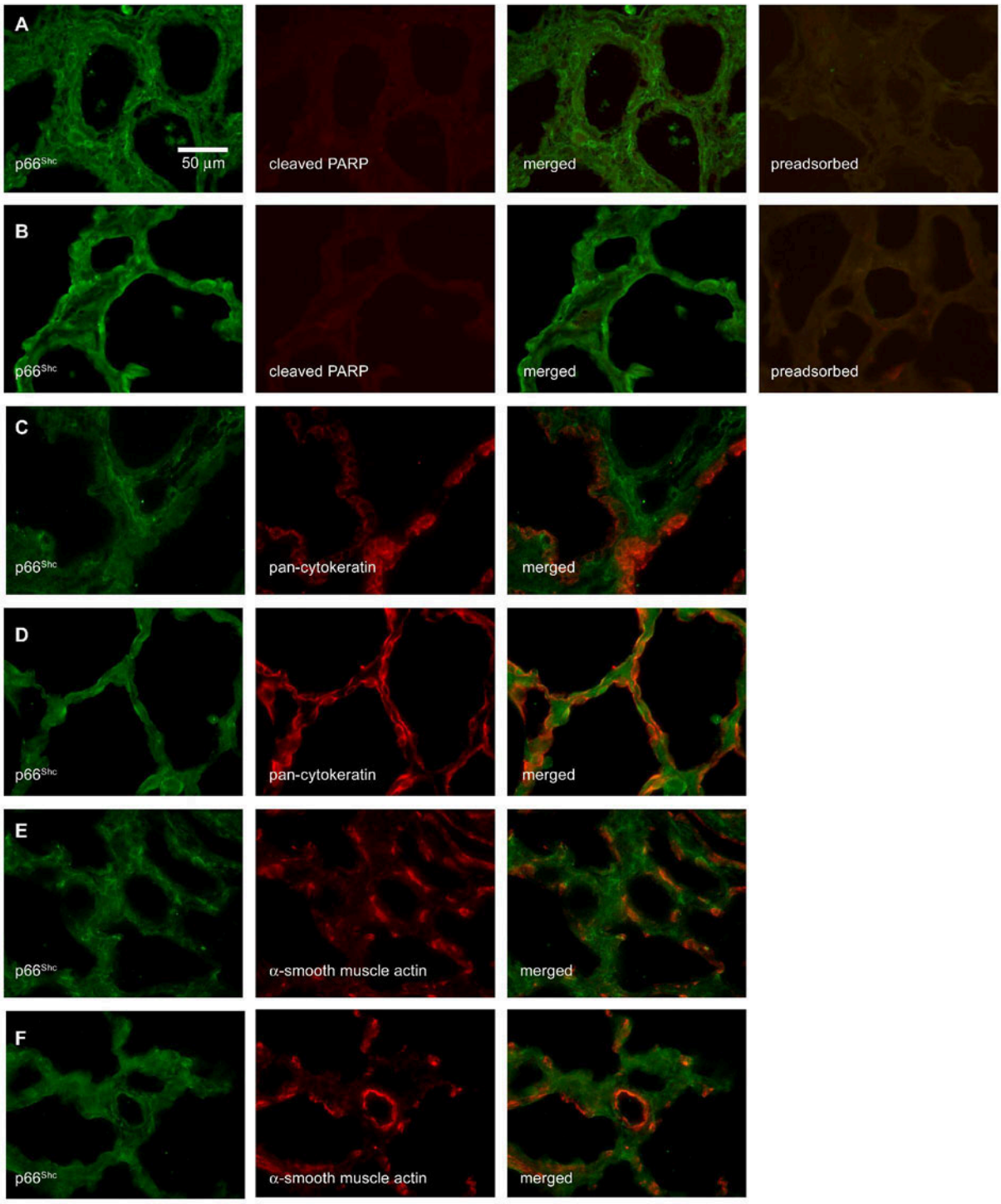
A
p66Shc
50 µm
cleaved PARP
merged
preadsorbed
B
p66Shc
cleaved PARP
merged
preadsorbed
C
p66Shc
pan-cytokeratin
merged
D
p66Shc
pan-cytokeratin
merged
E
p66Shc
α-smooth muscle actin
merged
F
p66Shc
α-smooth muscle actin
merged

Figure E3

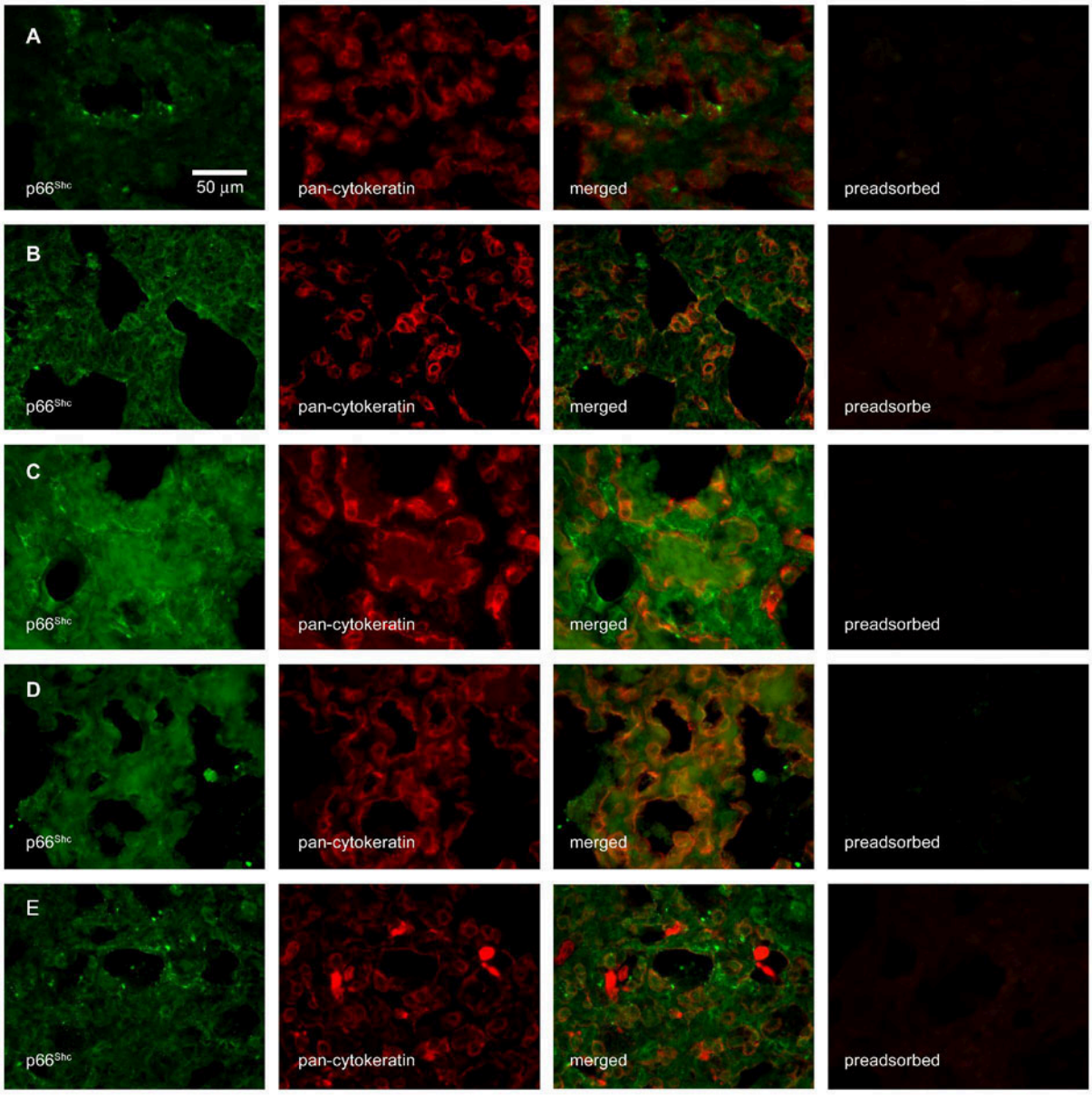
A
p66Shc
50 µm
pan-cytokeratin
merged
preadsorbed
B
p66Shc
pan-cytokeratin
merged
preadsorbe
C
p66Shc
pan-cytokeratin
merged
preadsorbed
D
p66Shc
pan-cytokeratin
merged
preadsorbed
E
p66Shc
pan-cytokeratin
merged
preadsorbed

Figure E4

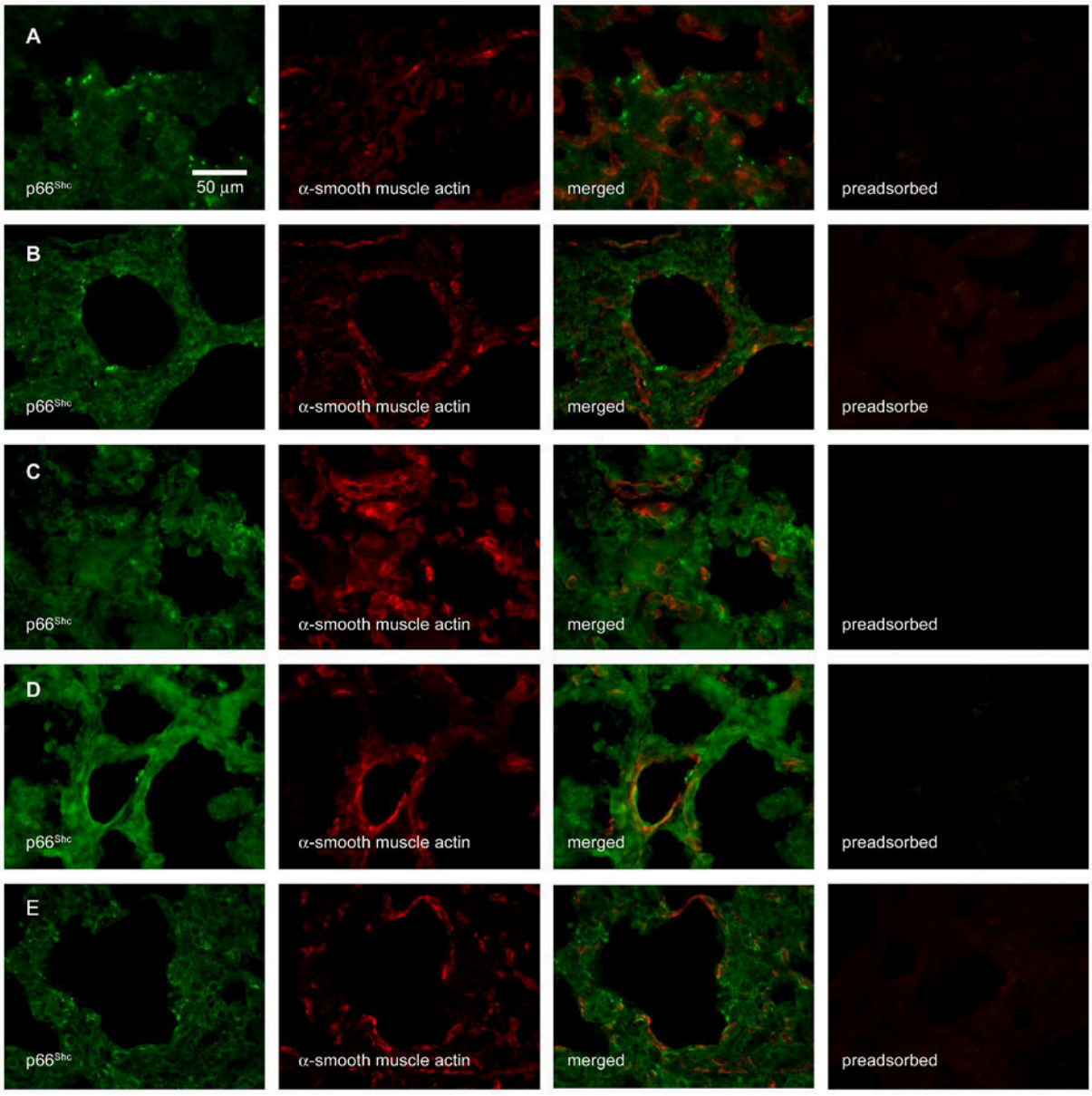
A
p66Shc
50 µm
α-smooth muscle actin
merged
preadsorbed
B
p66Shc
α-smooth muscle actin
merged
preadsorbe
C
p66Shc
α-smooth muscle actin
merged
preadsorbed
D
p66Shc
α-smooth muscle actin
merged
preadsorbed
E
p66Shc
α-smooth muscle actin
merged
preadsorbed

Figure E5

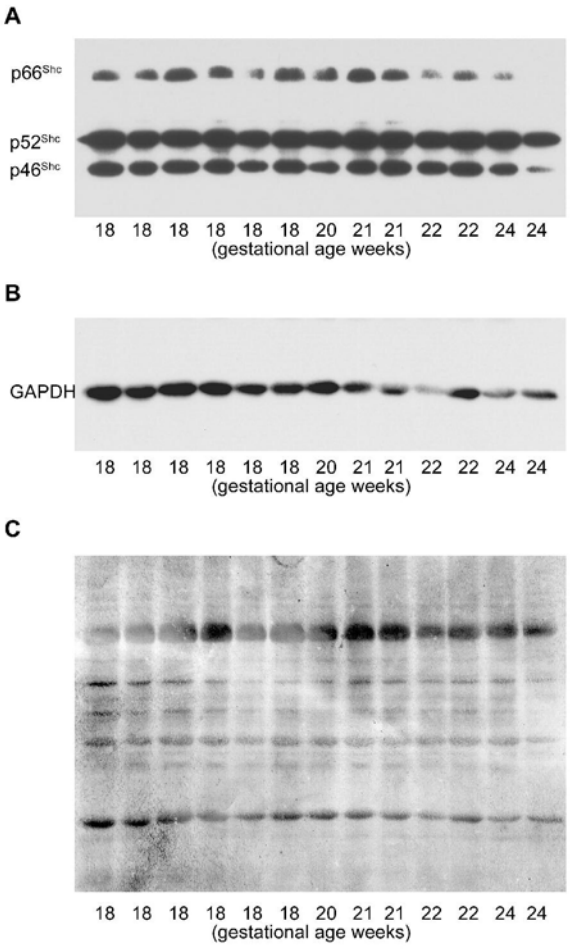
A
p66Shc
p52Shc
p46Shc
18 18 18 18 18 18 20 21 21 22 22 24 24
(gestational age weeks)
B
GAPDH
18 18 18 18 18 18 20 21 21 22 22 24 24
(gestational age weeks)
C
18 18 18 18 18 18 20 21 21 22 22 24 24
(gestational age weeks)

Figure E6

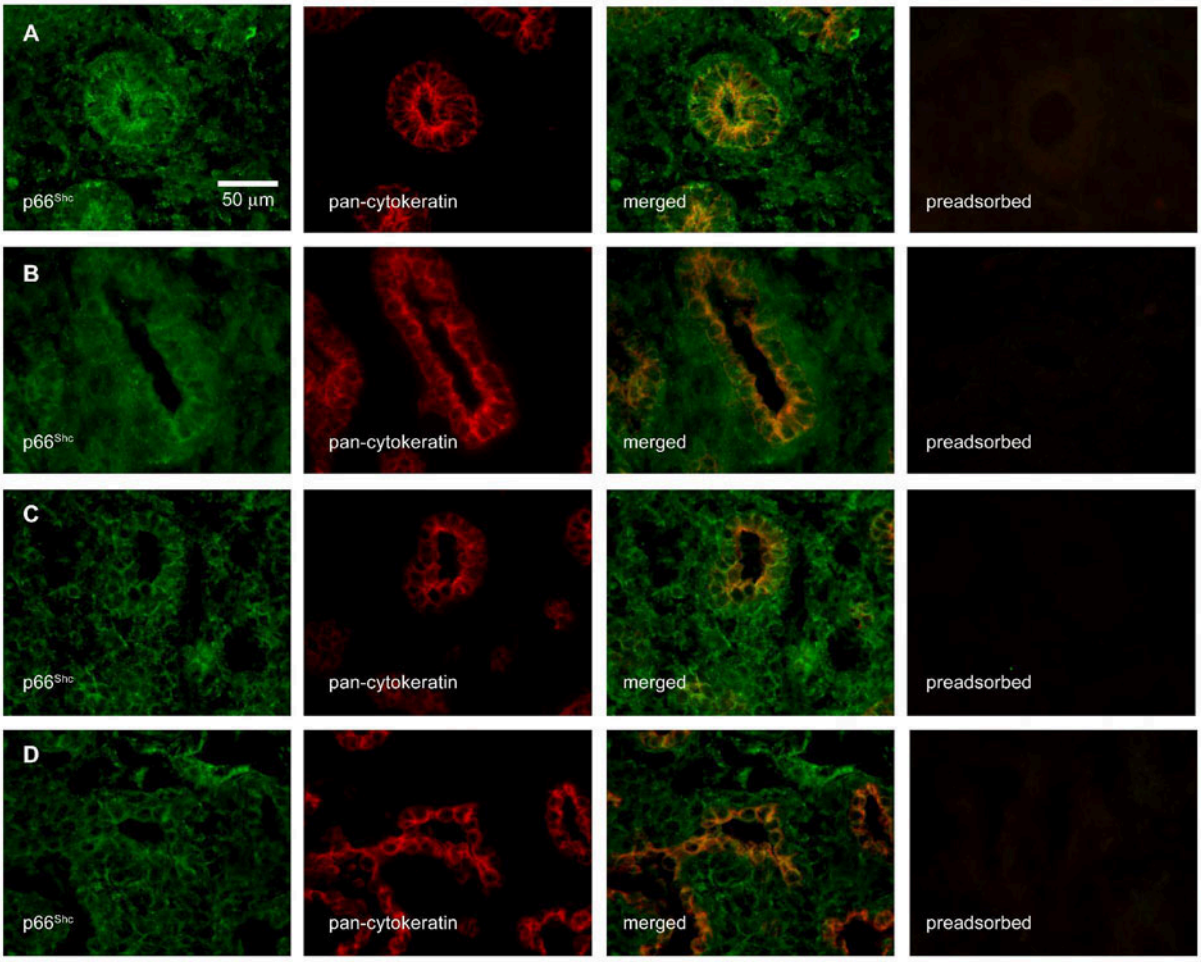
A
p66Shc
50 µm
pan-cytokeratin
merged
preadsorbed
B
p66Shc
pan-cytokeratin
merged
preadsorbed
C
p66Shc
pan-cytokeratin
merged
preadsorbed
D
p66Shc
pan-cytokeratin
merged
preadsorbed

Figure E7

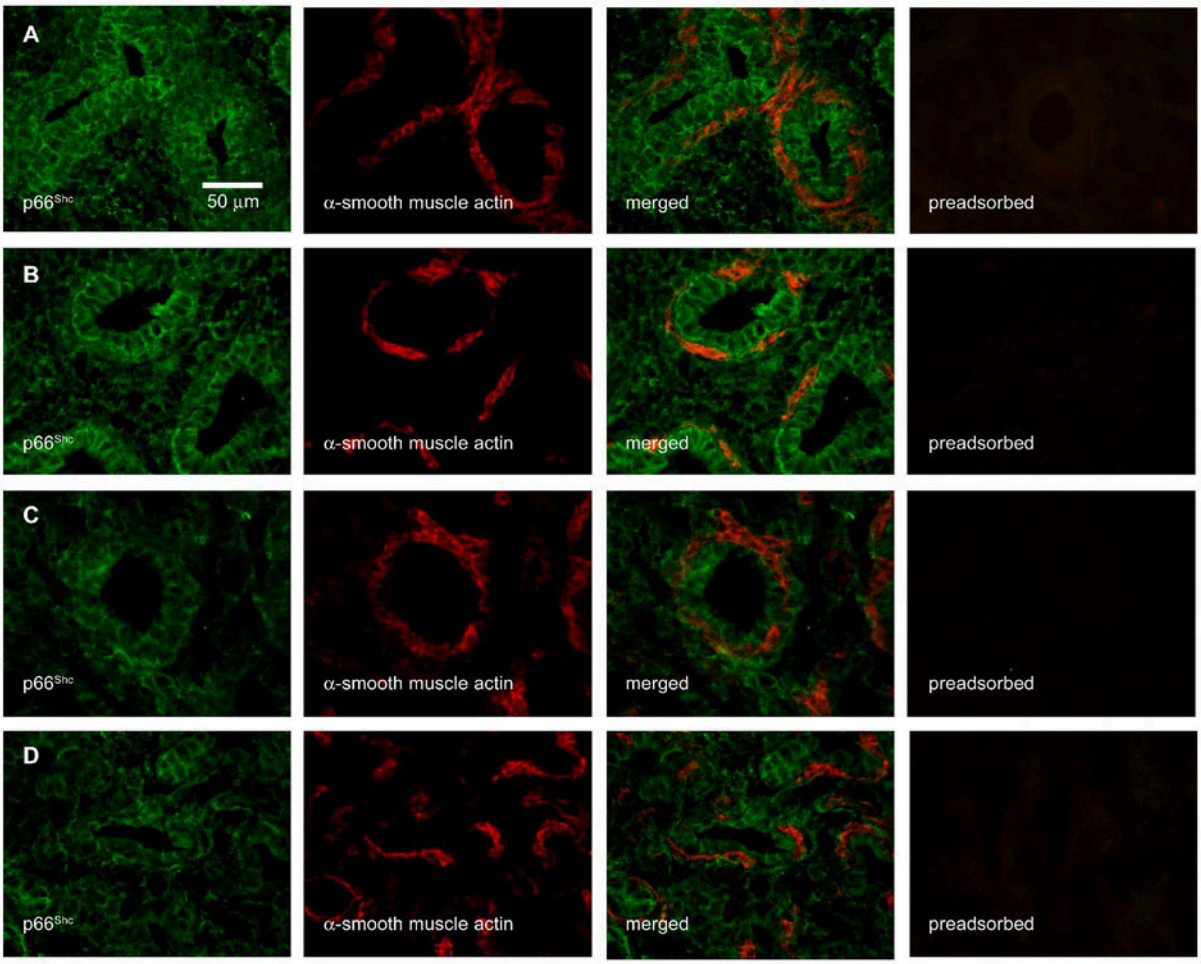
A
p66Shc
50 µm
α-smooth muscle actin
merged
preadsorbed
B
p66Shc
α-smooth muscle actin
merged
preadsorbed
C
p66Shc
α-smooth muscle actin
merged
preadsorbed
D
p66Shc
α-smooth muscle actin
merged
preadsorbed

Figure E8

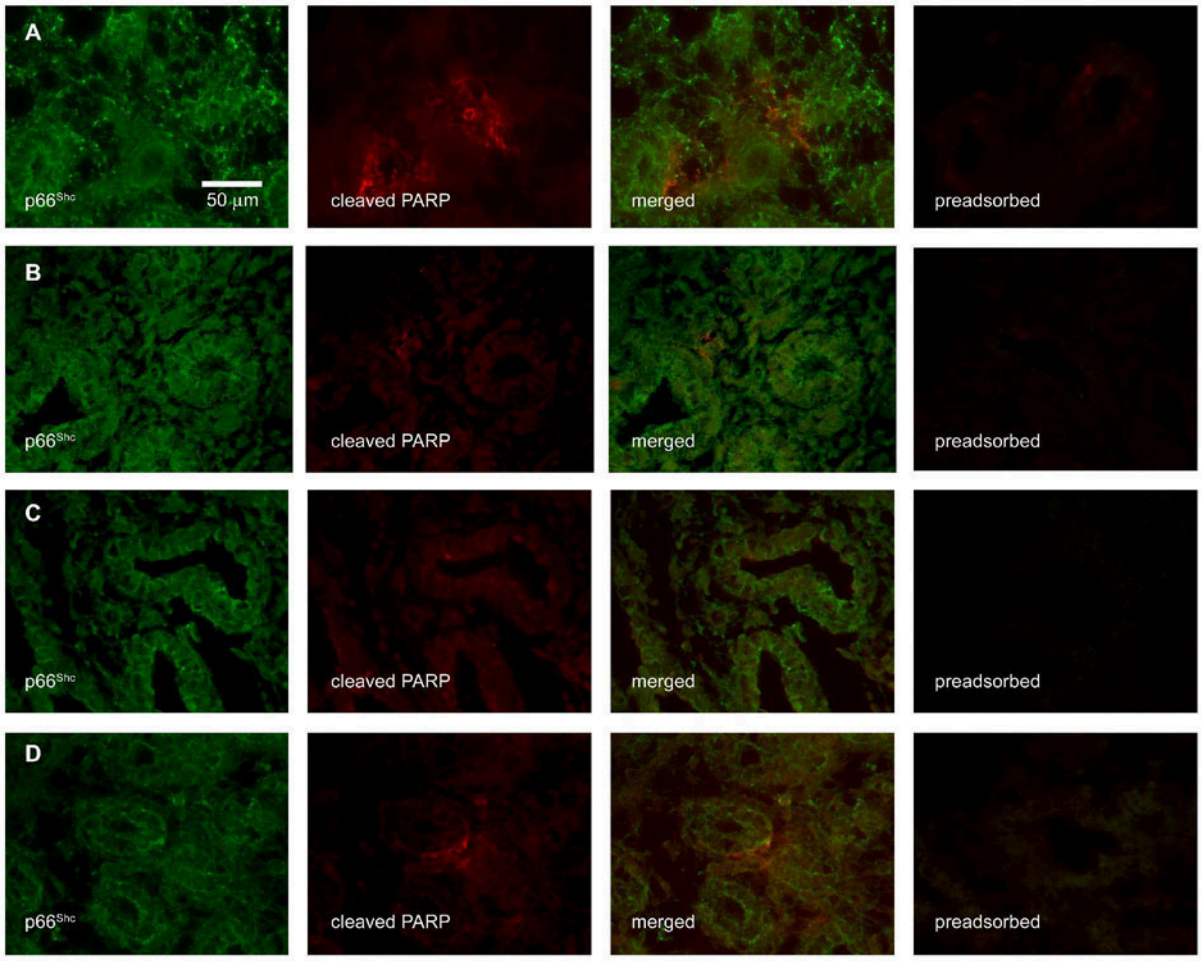
A
p66Shc
50 µm
cleaved PARP
merged
preadsorbed
B
p66Shc
cleaved PARP
merged
preadsorbed
C
p66Shc
cleaved PARP
merged
preadsorbed
D
p66Shc
cleaved PARP
merged
preadsorbed

Figure E9

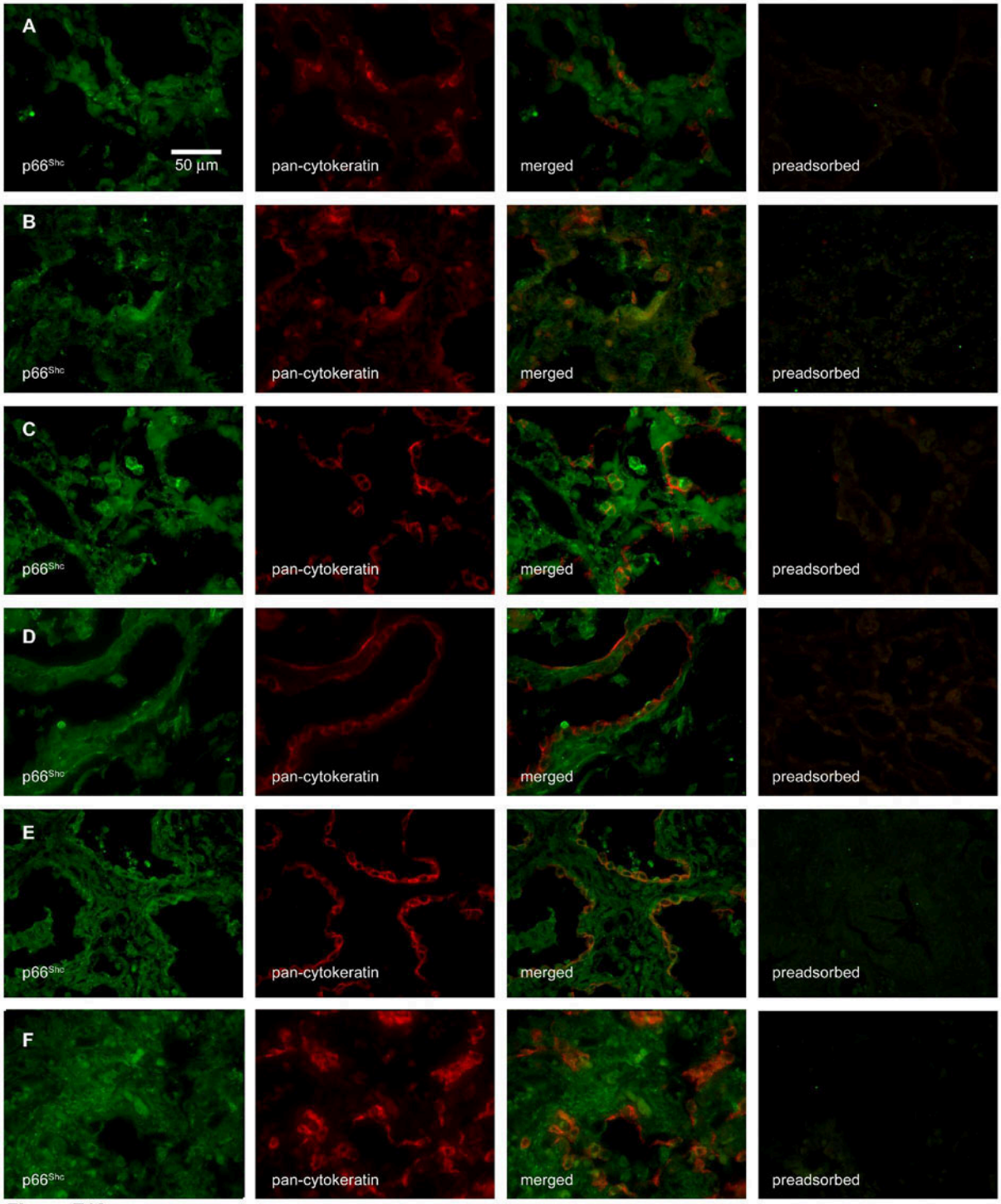
A
p66Shc
50 µm
pan-cytokeratin
merged
preadsorbed
B
p66Shc
pan-cytokeratin
merged
preadsorbed
C
p66Shc
pan-cytokeratin
merged
preadsorbed
D
p66Shc
pan-cytokeratin
merged
preadsorbed
E
p66Shc
pan-cytokeratin
merged
preadsorbed
F
p66Shc
pan-cytokeratin
merged
preadsorbed

Figure E10

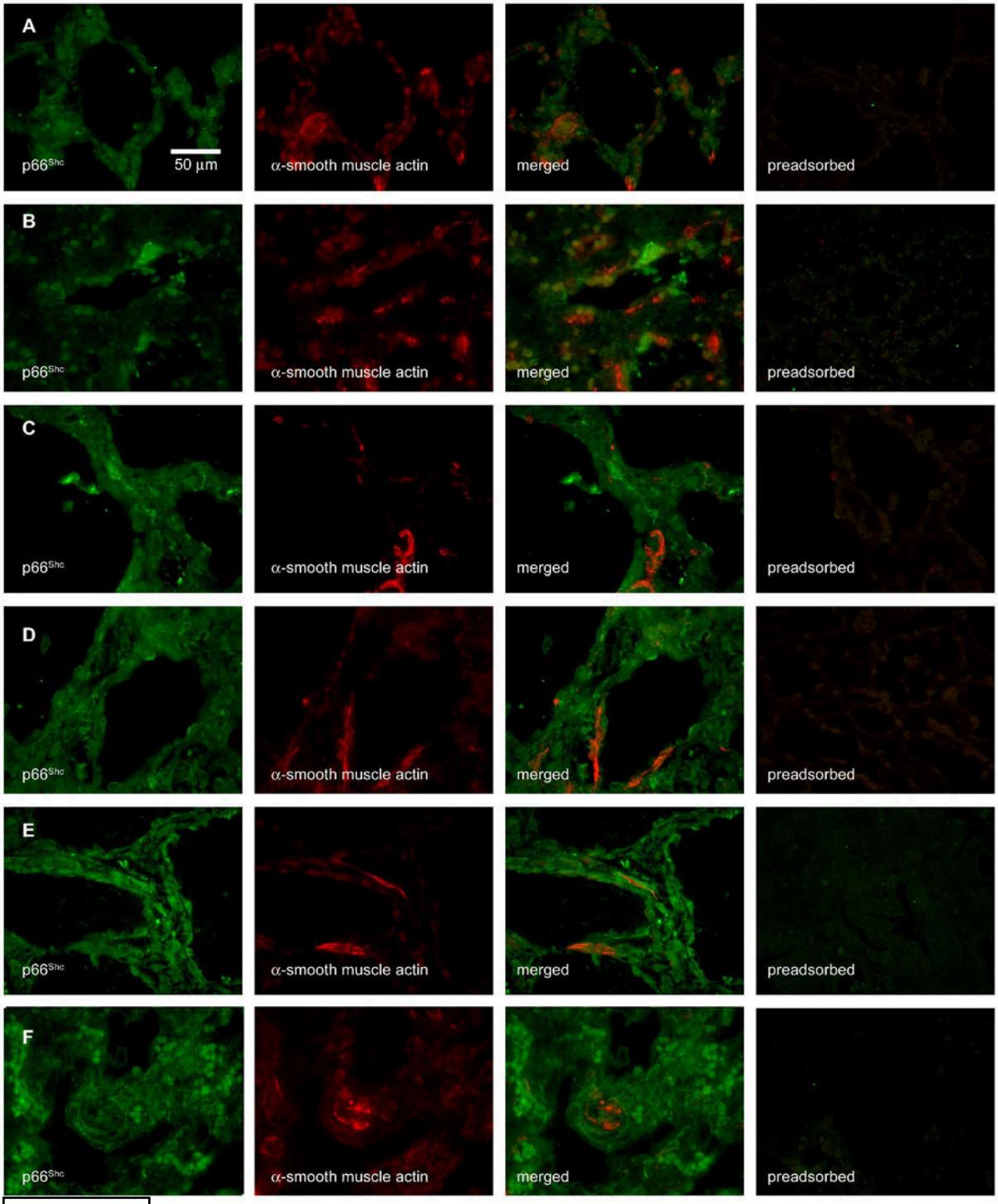
A
p66Shc
50 µm
α-smooth muscle actin
merged
preadsorbed
B
p66Shc
α-smooth muscle actin
merged
preadsorbed
C
p66Shc
α-smooth muscle actin
merged
preadsorbed
D
p66Shc
α-smooth muscle actin
merged
preadsorbed
E
p66Shc
α-smooth muscle actin
merged
preadsorbed
F
p66Shc
α-smooth muscle actin
merged
preadsorbed

Figure E11